Characteristics of Retinal Neovascularization in Proliferative Diabetic Retinopathy Imaged by Optical Coherence Tomography Angiography

Akihiro Ishibazawa,[1] Taiji Nagaoka,[1] Harumasa Yokota,[1] Atsushi Takahashi,[1] Tsuneaki Omae,[1] Young-Seok Song,[1] Tatsuhisa Takahashi,[2] and Akitoshi Yoshida[1]

[1]Department of Ophthalmology, Asahikawa Medical University, Asahikawa, Japan
[2]Department of Mathematical Information Science, Asahikawa Medical University, Asahikawa, Japan

Correspondence: Akihiro Ishibazawa, Department of Ophthalmology, Asahikawa Medical University, Midorigaoka Higashi 2-1-1-1, Asahikawa 078-8510, Japan; bazawa14@asahikawa-med.ac.jp.

Submitted: June 28, 2016
Accepted: October 17, 2016

Citation: Ishibazawa A, Nagaoka T, Yokota H, et al. Characteristics of retinal neovascularization in proliferative diabetic retinopathy imaged by optical coherence tomography angiography. *Invest Ophthalmol Vis Sci*. 2016;57:6247–6255. DOI:10.1167/iovs.16-20210

Purpose. To characterize the morphology of neovascularization at the disc (NVD) and neovascularization elsewhere (NVE) in treatment-naïve or previously treated proliferative diabetic retinopathy (PDR) patients using optical coherence tomography (OCT) angiography.

Methods. En face OCT angiograms of NVD/NVE in 40 eyes of 33 patients with PDR were acquired using RTVue XR Avanti OCT. The morphology of NVD/NVE on OCT angiograms was evaluated, and the activity was determined by biomicroscopy and fluorescein angiography (FA). In 12 eyes that were treated or treatment-naïve, changes in the morphology and vessel area of NVD/NVE before and after panretinal photocoagulation (PRP) were investigated.

Results. Twenty eyes had treatment-naïve PDR, whereas 20 eyes were previously treated with PRP. All treatment-naïve NVD/NVE had remarkable (i.e., active) leakage in early-phase FA. Ninety-five percent of treatment-naïve NVD/NVE observed by OCT angiography had exuberant vascular proliferation (EVP), identified as irregular proliferation of fine (smaller-caliber) new vessels; whereas, the presence of EVP in previously treated eyes (13/20) was significantly less than in treatment-naïve eyes (65% vs. 95%, $P = 0.043$). The remaining seven treated eyes had pruned NVD/NVE without EVP, observed as fibrotic changes or faint (inactive) leakage in FA. The vessel areas of NVD/NVE significantly decreased following PRP ($n = 12$, $P = 0.019$), and NVD/NVE morphology showed pruning and decreased EVP.

Conclusions. Exuberant vascular proliferation on OCT angiograms should be considered as an active sign of neovascularization; therefore, morphologic evaluation of neovascularization using OCT angiography may be useful to estimate the activity of each neovascularization in eyes with PDR.

Keywords: optical coherence tomography, optical coherence tomography angiography, neovascularization, diabetic retinopathy

The hallmark of proliferative diabetic retinopathy (PDR) is neovascularization that occurs at the vitreoretinal interface. Neovascularization is often associated with tractional retinal detachment and vitreous hemorrhage, which are leading causes of visual loss in patients with diabetes. It is observed on fundus biomicroscopy as small and/or large new vessels creating irregular vascular networks either on the retinal surface or protruding into the vitreous cavity.[1] However, the contrast between the new vessels and background fundus structures, such as intraretinal microvascular abnormality (IRMA) or laser scars, is occasionally fuzzy when closely monitoring the morphologic changes in neovascularization at the microcirculation level. In the landmark clinical trials of the Diabetic Retinopathy Study and Early Treatment Diabetic Retinopathy Study (ETDRS), fluorescein angiography (FA) was used as an adjunct for classifying disease severity, evaluating the degree of macular edema, and guiding laser therapy.[2–4] But in actual clinical practice, FA is a useful modality not only to detect neovascularization, but also to ascertain the activity of the neovascularization. However, FA is an invasive and time-consuming examination, and, therefore, it is not frequently performed.

Optical coherence tomography (OCT) is a noninvasive technique that provides cross-sectional retinal imaging and has been used clinically to diagnose and follow structural changes, such as macular edema, in diabetic retinopathy.[5] Several groups have reported features of neovascularization at the disc (NVD) and neovascularization elsewhere (NVE), as well as the associated changes at the vitreoretinal interface, using cross-sectional OCT images.[6–10] However, B-scan OCT images cannot directly visualize newly formed vessels; thus, concise morphologic evaluation of NVD and NVE remains restricted.

Recently developed OCT angiography techniques are gaining popularity for use in three-dimensional noninvasive chorioretinal vascular imaging.[11–25] Without the effect of fluorescein leakage, en face OCT angiography can clearly visualize the microvascular structures of neovascularization. This was shown in a study by Kuehlewein et al.,[18] who described two distinct morphologic patterns of type 1 choroidal neovascularization (CNV): new vessels radiated in a

branching pattern either in all directions from the center of the lesion (medusa pattern) or from one side of the lesion (sea fan pattern). Several authors have clearly shown neovascularization in PDR using en face OCT angiography.[19–23] We also recently reported the regression and pruning of NVD with remarkably proliferative microvessels following the intravitreous injection of anti-VEGF.[24] Spaide[25] described the signs of vascular abnormalities in CNV after anti-VEGF therapy observed by OCT angiography; however, morphologic assessment of neovascularization in PDR remains to be elucidated. In this study, we evaluated the characteristics of NVD and NVE in eyes with PDR using OCT angiography and FA to determine the correlation between the morphologic signs and the activity of NVD/NVE.

Methods

Study Population and Data Collection

This cross-sectional observational study was conducted at Asahikawa Medical University between December 1, 2014, and March 8, 2016. The study was performed in adherence with the tenets of the Declaration of Helsinki and was approved by the institutional review board of the Asahikawa Medical University. All subjects provided informed consent to participate in this research. Inclusion criteria involved new or previous diagnosis of PDR based on the International Clinical Diabetic Retinopathy and Diabetic Macula Edema Disease Severity Scales[26] and high-quality OCT angiograms of retinal neovascularization recorded during the study period. High-quality OCT angiograms were defined by a signal strength of at least 60. All patients underwent comprehensive ophthalmologic examination, including measurement of the best-corrected visual acuity (BCVA), IOP, slit-lamp biomicroscopy, color fundus photography, and OCT. Central macular thickness was measured using the ETDRS foveal central subfield by macular OCT. The following systemic clinical data were also recorded for all subjects at the time of ophthalmic examination: body mass index, blood pressure, hemoglobin A1c (HbA1c) level, and duration of diabetes. Patients with any other retinal disorders, including history of vitreous surgery and the presence of media opacities, such as severe vitreous hemorrhage and cataract, were not included. Patients who previously received intravitreous injection of anti-VEGF drugs also were excluded. The classification of new vessels was based on location; NVD was defined as new vessels located at the disc or within 1 disc diameter from its margin, and NVE was defined as new vessels located outside this area.[1] In patients with several new vessels in either eye, only one new vessel that could be scanned with OCT angiography was enrolled in this study.

In all treatment-naïve patients ($n = 14$), FA was performed using Spectralis HRA + OCT (Heidelberg Engineering, Heidelberg, Germany). Nineteen patients who were previously diagnosed with PDR received panretinal photocoagulation (PRP). Most treated patients ($n = 16$) also were examined by FA; however, two patients with severe renal failure and one patient with fluorescein allergy did not undergo FA.

En Face OCT Angiography

All patients were imaged using the commercially available spectral-domain OCT (RTVue XR Avanti; Optovue, Fremont, CA, USA) with AngioVue software (Optovue) to obtain en face OCT angiograms as previously described.[24] This OCT system operates at 70,000 A-scans per second to create 3×3 mm and 4.5×4.5 mm OCT angiograms consisting of 304×304 A-scans in approximately 2.9 seconds. The instrument has an axial resolution of 5 μm and a lateral resolution of 15 μm with an imaging range of 2 to 3 mm in the tissue. Each OCT angiogram was created using orthogonal registration and by merging two consecutive scan volumes. En face OCT angiograms (3×3 mm) were obtained from adjacent regions of the posterior pole, including NVE, by moving the software scanning area without changing the fixation using the Angio Retina mode. For assessment of NVD and NVE near the disc, OCT angiograms (3×3 mm or 4.5×4.5 mm) were obtained from the region around the optic disc using the Angio Disc mode. The scanning area was guided by the fundus observation of obvious fibrovascular membrane with slit-lamp biomicroscopy and/or the leakage in FA. We also confirmed the presence of new vessels using the B-scan OCT images with overlaying flow signal: the new vessels were observed as the structures with positive flow signal existing either on the retinal surface or protruding into the vitreous cavity. To best visualize new vessels on each en face OCT angiogram, segmentation of the inner border on the B-scan was manually moved at the vitreous cavity above the new vessels, whereas that of the outer border was manually adjusted just below the internal limiting membrane (ILM) to minimize the depiction of superficial vascular plexus.

Morphologic and Quantitative Evaluation of New Vessels

On en face OCT angiograms, the structural characteristics of new vessels and vascular flow areas of NVD and NVE were evaluated. The flow area was calculated by multiplying the number of pixels for which the decorrelation value was above that of the background with the pixel size, using the contained software (RTVue, version 2015.100.0.35; Optovue) as previously described.[24] In 12 previously treated or treatment-naïve eyes with NVD and NVE, the flow areas of new vessels before and 2 months after the start of PRP were measured from the same areas using en face OCT angiograms with the same segmentation boundaries. Measurements of the flow area represented the average of values captured by two observers (Y. S., H. Y.), who were masked to the clinical status of patients at the time of measurements.

Statistical Analysis

All data were expressed as the mean ± SD. The Mann-Whitney U test was used for statistical analysis of continuous variables, and the χ^2 test or Fisher's exact test was used for categorical variables. The Wilcoxon signed-rank test was used to compare flow areas before PRP with those after PRP in 12 eyes. SPSS statistics software version 19.0 (SPSS; Chicago, IL, USA) was used for statistical analysis, and $P < 0.05$ was considered statistically significant.

Results

Baseline Characteristics

A total of 40 eyes with PDR in 33 patients (22 males and 11 females) were included in this study. The patients ranged in age from 32 to 74 years, with a mean age of 52.5 years. Twenty eyes in 14 patients were treatment-naïve, and 20 eyes in 19 patients had been previously treated with PRP. The demographic and clinical characteristics of treatment-naïve and previously treated patients are shown in the Table. There were no significant differences in body mass index, blood pressure, HbA1c, and duration of diabetes between the groups. The BCVA in treatment-naïve eyes was higher than that in treated

eyes; however, the difference did not reach statistical significance ($P = 0.067$). The intervals between PRP in treated eyes and study enrollment ranged from 6 months to 20 years.

Characteristic OCT Angiography Features of Retinal Neovascularization

In fundus biomicroscopy, new vessels were observed as irregular red blood columns on the optic nerve head and the retinal surface, or protruding into the vitreous cavity; however, their detailed structures were not seen clearly because of the background retinal structures and laser scars (Figs. 1A, 1D). On en face OCT angiograms, two distinct morphologic features of new vessels were identified. First, most new vessels had the lesions with irregular proliferation of fine vessels, which were defined as exuberant vascular proliferation (EVP) (Fig. 1B). The second type of new vessels had pruned vascular loops of filamentous new vessels, but not EVP (Fig. 1E).

Relationship Between OCT Angiography Features and Fluorescein Leakage From Retinal Neovascularization in Treatment-Naïve or Previously Treated Eyes

In treatment-naïve eyes ($n = 20$), FA showed extensive leakage from all sites of NVD/NVE, even in the early phase (from 30 seconds to 1 minute). Consequently, 19 NVD/NVE sites (95%) had EVP (Fig. 2). In contrast, 13 (65%) of previously treated eyes ($n = 20$) had EVP with ongoing active leakage in FA (Fig. 3). Statistically, the number of treatment-naïve eyes with EVP in new vessels was significantly higher than that in previously treated eyes ($P = 0.043$; Table). Conversely, seven (35%) previously treated eyes had pruned vascular loops with no EVP by en face OCT angiography. These new vessels were observed as whitish fibrovascular membranes by fundus examination. Four eyes in which FA could be performed had faint leakage from pruned new vessels without EVP during the early phase of FA (Fig. 4).

New vessels in all 36 eyes that were examined with FA showed leakage in the late phase (approximately 5 minutes). Conversely, all NVD/NVE sites with EVP (30/30; 100%) had active leakage in the early phase, whereas most NVD/NVE sites without EVP (5/6; 83.3%) had only faint leakage; the number of new vessels with active leakage in early-phase FA was significantly higher in NVD/NVE sites with EVP than in those without EVP (Supplementary Table S1; $P = 0.000016$). The sensitivity and specificity of detecting EVP on active leakage in early-phase FA were 96.8% (30/31) and 100% (5/5), respectively. No significant differences in age, body mass index, blood pressure, HbA1c levels, duration of diabetes, BCVA, IOP, and central macular thickness were found between the eyes with EVP and those without EVP. However, among those eyes with NVD/NVE that were previously treated ($n = 20$), the mean duration after PRP was significantly shorter in eyes with EVP than in those without EVP (3.1 ± 4.3 years, $n = 13$ vs. 11.1 ± 7.6 years, $n = 7$; $P = 0.026$).

Changes in Retinal Neovascularization After Panretinal Photocoagulation

In eight treatment-naïve eyes and four previously treated eyes that still showed active new vessels, all of which had EVP, follow-up OCT angiograms were obtained 2 months after the start of PRP or after additional photocoagulation, respectively. Morphologically, pruning of new vessels and reduction in EVP were observed after the treatment (Figs. 5, 6). Additionally, the mean flow area of new vessels decreased significantly from

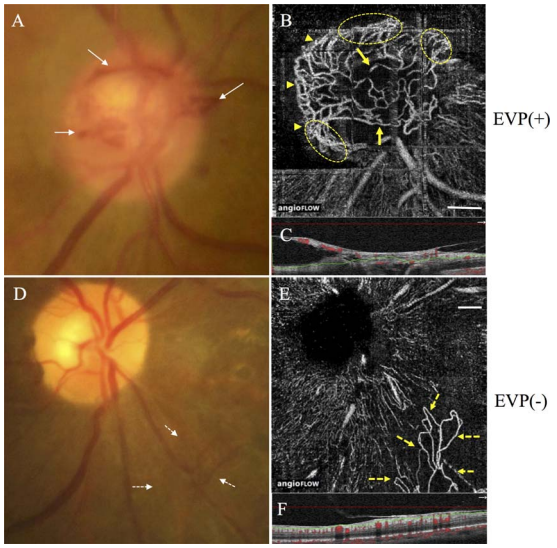

Figure 1. Optical coherence tomography angiography showing new vessel with two distinct morphologies. (**A**) Neovascularization at the disc in a 57-year-old female with treatment-naïve PDR. Abnormal red blood columns can be observed on the optic nerve head (*white arrows*), but their detailed morphology cannot be seen clearly. (**B**) An OCT angiogram of the optic disc vividly shows the morphology of the NVD; that is, large-trunk vessels (*yellow arrows*), terminal loops, and anastomotic connections at the outer border of neovascularization (*arrowheads*). The most distinguishing feature of this type of neovascularization is EVP, which can be identified as irregular proliferation of small-caliber new vessels (*ellipses*). *Scale bar*: 0.5 mm. (**C**) A horizontal B-scan image shows layer segmentation of the corresponding en face OCT angiogram shown on (**B**). (**D**) Another case of NVD in a 53-year-old male with clinically inactive PDR treated with panretinal photocoagulation 1 year ago. New vessels near the nasal side of the disc can be seen faintly (*white-dot arrows*), but their structures are not identified distinctly because of background retinal structures and laser scars. (**E**) An OCT angiogram of the optic disc clearly shows the NVD has pruned vascular loops of filamentous new vessels (*arrows*) but does not have lesions of EVP. *Scale bar*: 0.5 mm. (**F**) A horizontal B-scan image shows layer segmentation of the corresponding en face OCT angiogram shown on (**E**). *Red* and *green lines* in (**C**) and (**F**) are the inner and outer segmentation boundaries for en face OCT angiograms, respectively.

0.70 ± 0.70 mm² to 0.47 ± 0.43 mm² after PRP ($n = 12$, $P = 0.019$). The flow area was decreased in all new vessels ($n = 11$) but one, in which the flow area of NVD was conversely increased after PRP (Fig. 6E).

Case Presentation

The time course of the treatment-naïve eye of a 51-year-old female with NVD that had increased flow area following PRP is presented in Figures 7 and 8. At the first visit, FA showed no apparent signs of NVD (Figs. 7A, 7B); however, OCT angiography revealed the presence of vascular sprouting at the temporal rim of the disc (Fig. 7C). After 3 months, vascular sprouts developed into NVD with some evidence of EVP (Fig. 7E). At that time, PRP treatment started developing in the inferior retina in a clockwise direction. One month later, NVD exhibited signs of pruning, and the lesions associated with EVP were decreased (Fig. 7G). Optical coherence tomography angiography performed at the end of 2 months of PRP showed that NVD had not disappeared, but had extended in a direction toward the macula (Fig. 7K). Montage OCT angiography of the optic disc and macula was created to examine the complete morphology of fibrovascular membrane, including new vessels

Investigative Ophthalmology & Visual Science

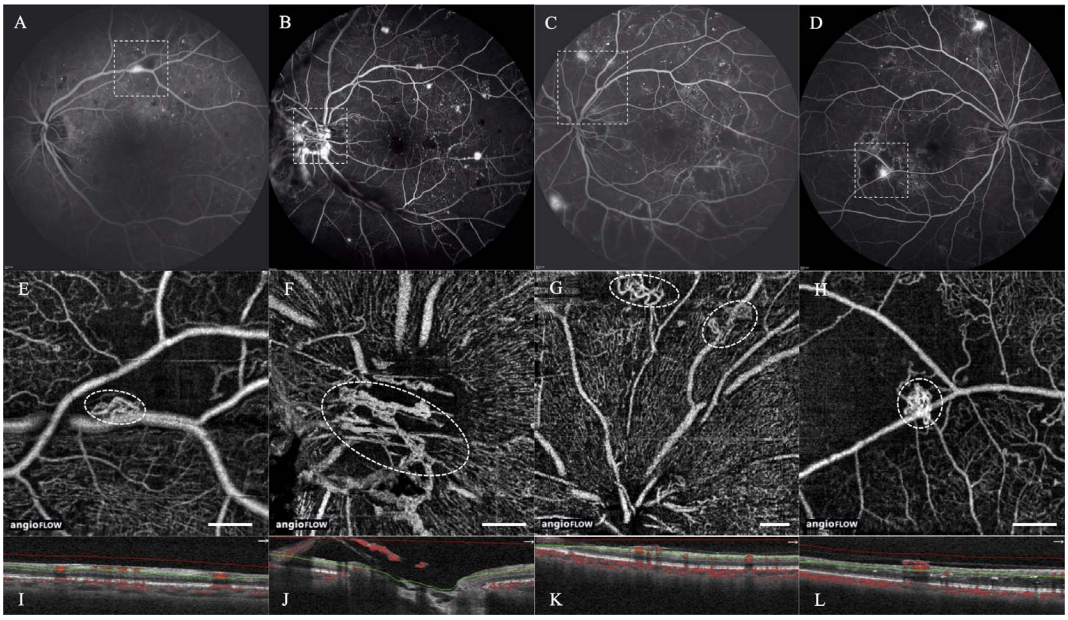

FIGURE 2. Four representative cases with treatment-naïve proliferative diabetic retinopathy. (**A–D**) Early-phase FA shows remarkable (i.e., active) leakage from NVD or NVE in a 71-year-old male, 52-year-old male, 46-year-old female, and a 60-year-old male, respectively. (**E–H**) Optical coherence tomography angiography images of 3 × 3 mm or 4.5 × 4.5 mm areas indicated within the *squares* in corresponding FA images shown on (**A**) to (**D**), respectively. All treatment-naïve NVD and NVE cases have EVP (*ellipses*), corresponding to the parts of active leakage in FA. *Scale bar*: 0.5 mm. (**I–L**) Horizontal B-scan images show layer segmentation of the corresponding en face OCT angiograms shown on (**E**) to (**H**), respectively. *Red* and *green lines* are the inner and outer boundaries, respectively.

5 months after the start of PRP (Fig. 8C). The original NVD was now a large-trunk vessel, and new vessels were pruned; however, additional new vessels with EVP were extending toward the macula.

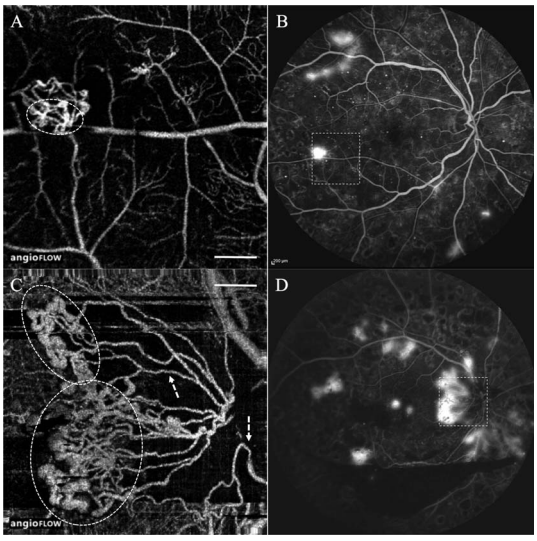

FIGURE 3. Representative cases with treated, albeit still active, PDR. (**A**) An OCT angiogram (3 × 3 mm) of NVE in the left eye of a 54-year-old female. The NVE has partial of EVP (*ellipse*). *Scale bar*: 0.5 mm. (**B**) Early-phase FA of the same eye. Remarkable leakage from several NVEs is observed. The *square* outlines the area shown in (**A**). (**C**) An OCT angiogram (3 × 3 mm) of NVD in the right eye of a 59-year-old male. The NVD has pruned large-trunk vessels (*dotted arrows*), saccular and dilated terminals, and anastomotic connection of outer borders. The NVD also exhibits EVP (*ellipses*). *Scale bar*: 0.5 mm. (**D**) Early-phase FA of the same eye. Remarkable leakage from the NVD and several NVEs and preretinal hemorrhage are observed. The *square* outlines the area shown in (**C**).

DISCUSSION

As we and others previously demonstrated,[19–24] en face OCT angiography can directly visualize well-delineated microvascular structures of new vessels and differentiate them from original retinal vascular structures. However, the detailed morphologic features of these newly formed vessels have not been extensively characterized. The current study revealed that new vessels in patients with PDR could be morphologically divided into two main types: new vessels with EVP and those without EVP (Fig. 1). EVP, which is the intense growth of irregular small-caliber vessels located at the margin of new vessels, likely represents active proliferation, as almost all treatment-naïve eyes with PDR (95%) had lesions with EVP (Fig. 2). In contrast, the rate of EVP in new vessels in eyes treated with PRP was 65%, and the remaining new vessels without EVP (35%) in these previously treated eyes had only filamentous vascular loops (Table; Figs. 3, 4). These looped structures without EVP detected by OCT angiography were observed as whitish fibrovascular membranes without obvious red blood columns by funduscopy. The degree of leakage in FA also strongly supported the conclusion that these were indeed active new vessels. A previous study clearly demonstrated that immature (i.e., young) neovascularization had a much faster and greater leakage of fluorescein than mature (old) neovascularization.[27] The current results demonstrated that all new vessels with EVP had excessive leakage in early-phase FA, whereas 83.3% of the new vessels without EVP had faint leakage. This concordance between the presence of EVP in OCT angiography and remarkable leakage in early-phase FA indicated that the presence of EVP on OCT angiograms should be interpreted as an active sign of new vessels in clinical practice.

Corresponding to the reduction in fluorescein leakage after PRP, new vessels with EVP before PRP were predictably pruned in the vascular area and signs of EVP were decreased (Figs. 5, 6). Moreover, the mean duration after PRP in eyes with

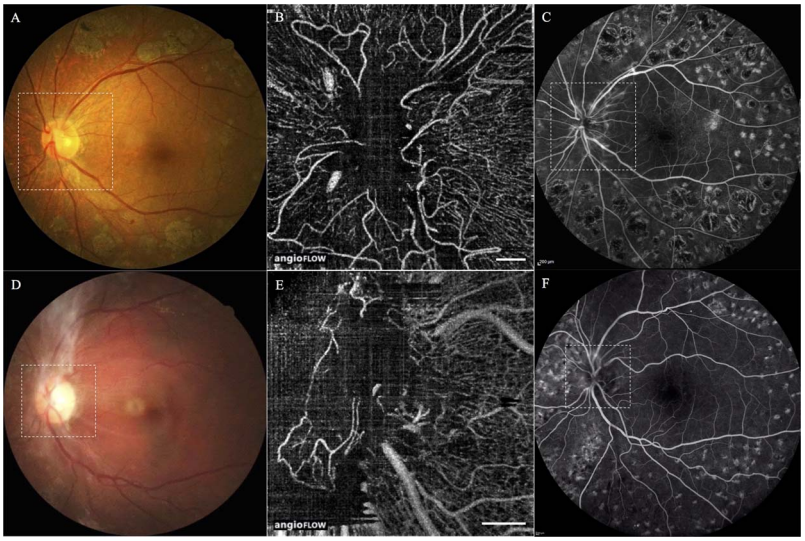

FIGURE 4. Representative cases with treated inactive PDR. (**A**) A color fundus photograph of the left eye of a 44-year-old male who received PRP 10 years ago. The *square* outlines the area shown in (**B**). (**B**) Optical coherence tomography angiography of a 4.5×4.5 mm area centered on the optic disc shows pruned NVD. There is no EVP. *Scale bar*: 0.5 mm. (**C**) Early-phase FA shows faint leakage from the NVD. The *square* outlines the area shown in (**B**). (**D**) A color fundus photograph of the left eye of a 62-year-old female who received PRP 9 years ago. Whitish fibrovascular membrane is observed. The *square* outlines the area shown in (**E**). (**E**) Optical coherence tomography angiogram of the 3×3 mm area centered on the optic disc shows pruned NVD. There is also no EVP. *Scale bar*: 0.5 mm. (**F**) Early-phase FA shows faint leakage from the NVD. The *square* outlines the area shown in (**E**).

EVP was significantly shorter than that in eyes without EVP. Previous studies clearly demonstrated that VEGF concentration in the ocular fluid of patients with active PDR was higher than that in patients with quiescent PDR,[28,29] and that VEGF levels decreased following successful laser photocoagulation.[28] Inhibition of VEGF by intravitreous injection of bevacizumab led to complete, or at least partial, resolution of leakage from new vessels in FA, with a concomitant reduction in the caliber or presence of perfused blood vessels.[30,31] Although we did not directly measure the VEGF concentrations in the ocular fluid of patients with PDR either before or after PRP in this study, we predicted that the VEGF concentrations after PRP treatment were decreased in parallel to decreased activity of new vessels and decreased EVP, as detected by OCT angiography.

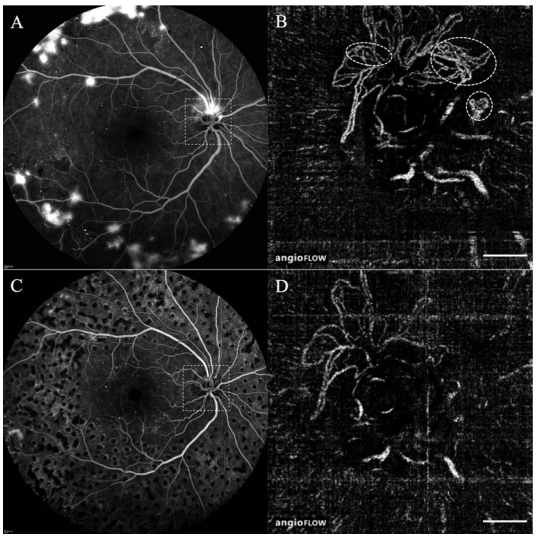

FIGURE 5. A representative case of a 48-year-old male with treatment-naïve PDR before and after PRP. (**A**) Early-phase FA before PRP shows remarkable leakage from NVD and numerous sites of NVE. The *square* outlines the area shown in (**B**). (**B**) Optical coherence tomography angiography in the 3×3 mm area centered on the optic disc clearly visualizes new vessels with lesions of EVP (*ellipse*). *Scale bar*: 0.5 mm. (**C**) Early-phase FA in the same eye 2 months after the start of PRP. Early leakage from NVD and NVEs are markedly diminished. The *square* outlines the area shown in (**D**). (**D**) Optical coherence tomography angiography after PRP shows pruned NVD and decreased lesions of EVP. *Scale bar*: 0.5 mm.

Previously reported histologic findings have provided evidence on the role of VEGF in the development of EVP; for example, an angio-fibrotic switch in PDR has previously been proposed by several studies.[32,33] Injection of anti-VEGF drugs could lead to a profibrotic switch with significant reduction in the neovascular component, as determined by decreased expression of the panendothelial marker CD34 and the marked increase in the contractile elements, smooth muscle actin and collagen, of the proliferative membrane over time.[33] These histologic findings provided evidence that EVP observed by OCT angiography might represent newly growing sections of active new vessels as they are significantly affected by VEGF inhibition. Conversely, pruned new vessels with no sign of EVP likely reflect the inactive fibrotic stage of neovascular membranes.

Furthermore, Spaide[25] recently evaluated the morphologic vascular abnormalities associated with periodic antiangiogenic therapy for CNV on OCT angiograms. He proposed that high levels of cytokines, such as VEGF, led to exuberant proliferation of new vessels (i.e., angiogenesis); however, after anti-VEGF injection, the levels of free VEGF dropped precipitously with subsequent regression of the newly growing vessels, particularly those with poor pericyte coverage. Some vessels with pericyte coverage remained, and arteriogenesis led to an increase in vascular diameter with increased blood flow through the remaining vessels. The consequent increase in VEGF and repeated inhibition of VEGF enhanced pruning of new vessels, leading to the formation of large-sized, abnormal anastomotic connections similar to those observed in shunt vessels.[25] These processes occurred in many blood vessels throughout the body and were likely to occur in new vessels in

Investigative Ophthalmology & Visual Science

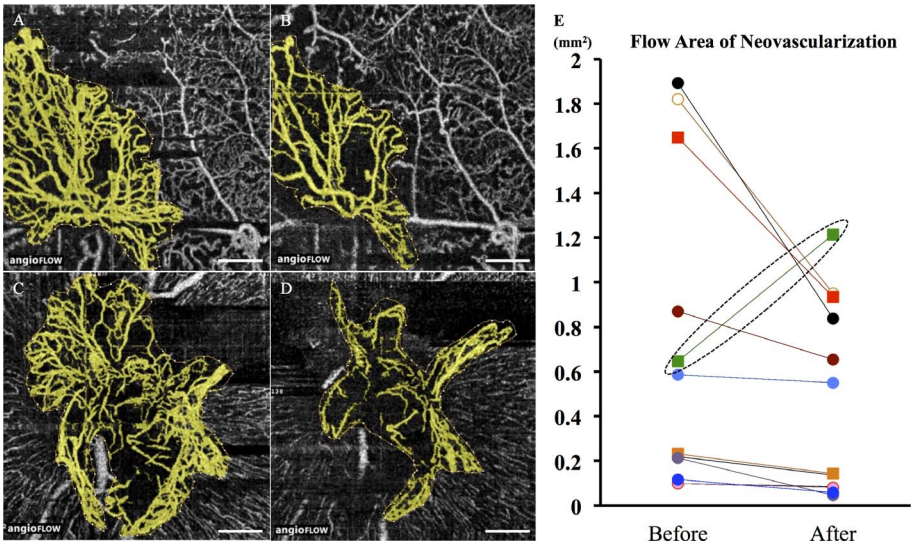

Figure 6. Quantitative evaluation of the flow areas of NVE and NVD by OCT angiograms before and after photocoagulation. (**A**, **B**) Optical coherence tomography angiograms of treatment-naïve NVE in a 49-year-old male. *Scale bar*: 0.5 mm. (**A**) Before PRP, the flow area of NVE was 1.82 mm^2. Exuberant vascular proliferation of NVE is present. (**B**) Two months after the start of PRP, the flow area is decreased to 0.95 mm^2. The NVE has less EVP and becomes pruned. (**C**, **D**) Optical coherence tomography angiograms of a treatment-naïve NVD in a 64-year-old man. *Scale bar*: 0.5 mm. (**C**) Before PRP, the flow area of NVD is 1.89 mm^2. The NVD has remarkable EVP. (**D**) Two months after the start of PRP, the flow area is decreased to 0.84 mm^2. The NVD has less EVP and becomes pruned. (**E**) The changes in the flow areas of NVE or NVD in each case ($n = 12$) before and 2 months after PRP. The flow areas are decreased in all cases but one; the flow area in that case is conversely increased after PRP (*circumscribed plots*).

the eyes of patients with PDR. Our current observations showing that new vessels with EVP were converted to pruned new vessels with residual, larger vascular loops after PRP suggested that new vessels in the eyes of patients with PDR might be at least partially undergoing these processes.

In the current study, for the first time, we circumstantially reported the growth process of NVD in PDR (Figs. 7, 8): OCT angiography clearly demonstrated a vascular bud merging with another bud to distinctively undergo neovascularization with concurrent signs of EVP. Vascular spouting observed in this case was very similar to that of NVE from the superficial capillaries in hemicentral retinal vein occlusion, as we previously described.[34] Moreover, the exuberant NVD was pruned after the start of PRP and became a large-trunk vessel, whereas additional new vessels growing toward the macula had EVP. This patient did not have posterior vitreous

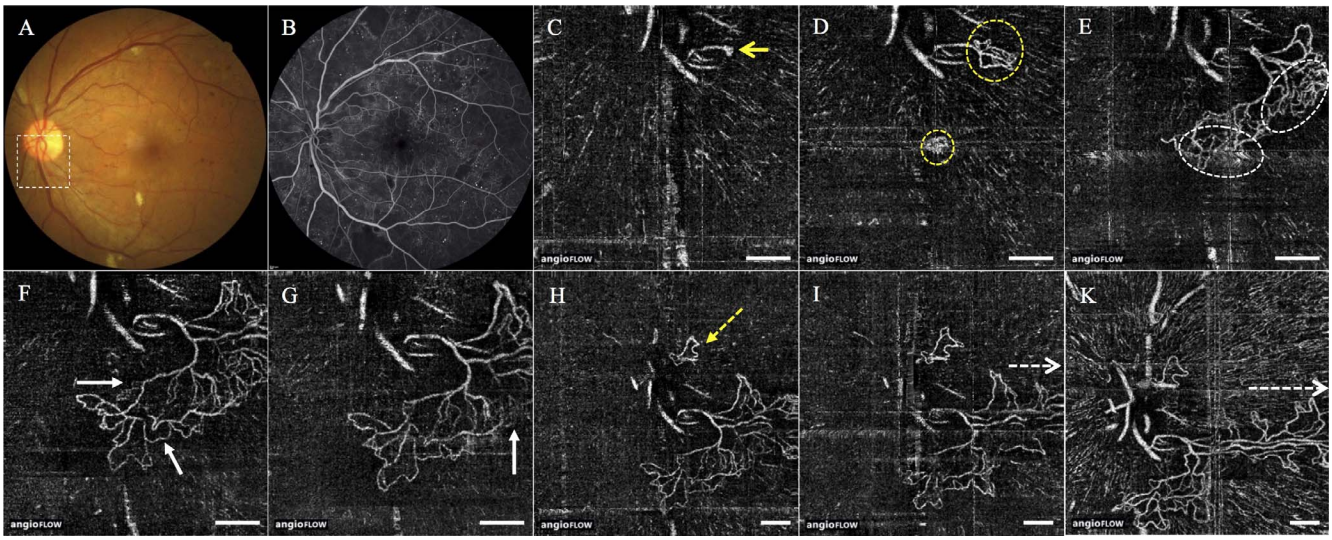

Figure 7. The left eye of a 51-year-old female with increased flow area of NVD after PRP shown on the graph in Figure 6. (**A**) A color fundus photograph at the first visit, the *square* outlines the area shown in the OCT angiograms below. (**B**) Early-phase FA shows no apparent sign of NVD. (**C**) Optical coherence tomography angiography (3 × 3 mm) reveals the presence of vascular sprout at the temporal rim of the disc (*yellow arrow*). (**D**) Six weeks later, OCT angiography shows the growing sprout with the appearance of another new vessel sprout (*yellow circles*). (**E**) Three months after the first visit, the sprouts develop into an NVD with parts of EVP (*white ellipses*). At this time, PRP treatment is started from the inferior retina in a clockwise direction. (**F**, **G**) Two weeks and 1 month later, respectively, the NVD becomes pruned and lesions with EVP are decreased (*white arrows*). (**H**) Two months later, PRP is completed, but OCT angiography (4.5 × 4.5 mm) shows that the NVD does not shrink, and that another new vessel has spouted at the upper rim of the disc (*yellow-dotted arrow*). (**I**, **K**) Three and 4 months later, respectively, the NVD becomes pruned but grows and extends toward the macula (*white-dotted arrows*). *Scale bar*: 0.5 mm in (**C**) to (**K**).

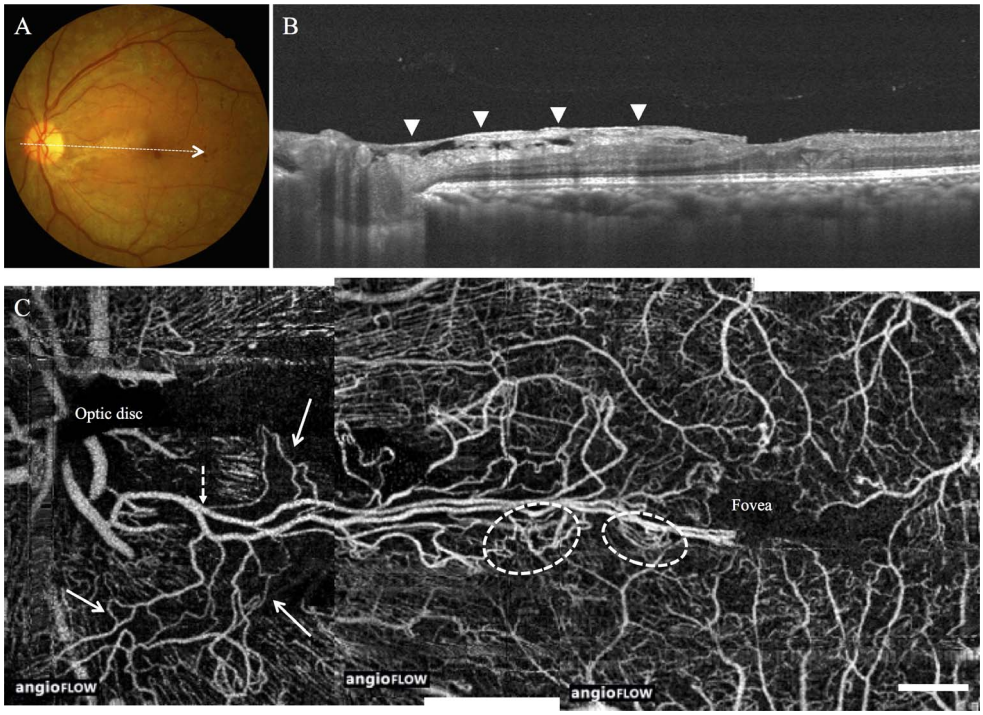

Figure 8. Images of the left eye of a 51-year-old female shown in Figure 7, 5 months after the start of PRP. (**A**) A color fundus photograph. *White-dotted arrow* indicates the location of *horizontal line* of OCT of (**B**). (**B**) A horizontal OCT B-scan. The *arrowheads* indicate the thick fibrovascular membrane growing from the optic disc and extending to the macula. Posterior vitreous detachment is not observed. (**C**) A montage image made from three OCT angiograms (3 × 3 mm) around the optic disc and macula. The original NVD has evolved into a large-trunk vessel (*dotted arrow*), and new vessels are pruned (*arrows*). However, new vessels growing toward the macula have sections with EVP (*ellipses*). *Scale bar*: 0.5 mm.

detachment; thus, we predicted that the growing NVD trailed the posterior hyaloid toward the macula where laser treatment was not performed.

This study has several limitations. First, in some instances, OCT angiogram images vaguely showed the vessels of the superficial vascular plexus and/or radial peripapillary capillaries. En face segmentation of the outer border on OCT angiograms was set just below the ILM as the default setting of vitreous slab on AngioVue software, because thin fibrovascular membranes including new vessels could occasionally be misidentified as the ILM. Differentiation between neovascularization and IRMA should be considered,[9] as IRMA usually has minimal or no leakage in FA.[35] In the current study, we confirmed the presence of overlaying flow signals on OCT B-

Table. Demographic and Clinical Characteristics of Treatment-Naïve and Previously Treated Patients

Variables	Treatment-Naïve, $n = 14$	Treated With PRP, $n = 19$	P
Age, y	52.7 ± 9.4	52.4 ± 11.8	0.55
Sex, *n* (%)			0.27
Male	11 (78.6)	11 (57.9)	
Female	3 (21.4)	8 (42.1)	
Body mass index	25.9 ± 4.1	26.9 ± 6.4	0.54
Blood pressure, mm Hg			
Systolic	151.4 ± 22.3	139.8 ± 28.3	0.13
Diastolic	85.8 ± 12.4	79.7 ± 14.4	0.21
Mean	107.7 ± 14.6	99.7 ± 16.8	0.23
HbA1c	8.6 ± 2.1	8.1 ± 1.8	0.45
Duration of diabetes, y	12.9 ± 9.7	14.7 ± 10.8	0.53
Enrolled eye, *n*	20	20	
Duration after PRP, y (range)	N/A	5.9 (0.5–20)	
BCVA, logMAR	0.08 ± 0.20	0.39 ± 0.45	0.067
IOP, mm Hg	16.8 ± 3.5	15.8 ± 3.5	0.55
Central macular thickness, μm	278.6 ± 51.0	333.9 ± 167.2	0.21
Enrolled neovascularization, *n* (%)			0.51
NVD	11 (55)	14 (70)	
NVE	9 (45)	6 (30)	
Presence of EVP, *n* (%)	19 (95)	13 (65)	0.043

scan images in structures breaching the ILM and/or the posterior hyaloid; therefore, the potential interference of IRMA in evaluation of the extent of NVD/NVE was minimized. Second, we did not perform FA in 37.5% (3/8) of the eyes that had looped new vessels without EVP on OCT angiograms. However, in those three eyes, pruned new vessels on OCT angiograms were observed as whitish fibrovascular membranes with no obvious red blood columns on fundoscopy and were clinically diagnosed as inactive new vessels.[1,10] A third limitation was the classification of buds (sprouts) of new vessels that could sometimes be detected using FA and OCT angiography. The morphology of the vascular buds observed with OCT angiography did not resemble an exuberant form, but instead was shaped like a tuft or a small loop; thus, buds could potentially have been classified as small new vessels without EVP in this study. However, vascular buds can sprout and grow into new vessels, as that was shown in our case (Fig. 7); thus, growing buds should be considered as active. The morphology of small new vessels by OCT angiography should be carefully evaluated, and might need to be supported with FA to determine the activity of particularly small new vessels especially. A fourth limitation was the very narrow field of view on 3 × 3 mm OCT angiography scans during screening for peripheral NVE. Although OCT angiography scans in the larger size of 6 × 6 mm can better visualize peripheral NVE,[23] the detailed features, such as the presence of EVP, are not clearly depicted due to low resolution. However, the development of wider and higher-resolution scans for OCT angiography should address this concern in the future.

In conclusion, en face OCT angiography allowed us to observe structures of retinal neovascularization at the microcirculation level and to evaluate the morphologic features of new vessels. Exuberant vascular proliferation observed in new vessels on OCT angiograms can be an active sign of neovascularization. Although a wider scan area is desired for future screening, morphologic evaluation of neovascularization using OCT angiography may be useful for clinicians to estimate the activity of each neovascularization in the eyes of patients with PDR.

Acknowledgments

Supported by a Grant-in-Aid for Scientific Research (B) 25293352 (TN) from the Japan Society for the Promotion of Science, Tokyo, Japan.

Disclosure: **A. Ishibazawa**, None; **T. Nagaoka**, None; **H. Yokota**, None; **A. Takahashi**, None; **T. Omae**, None; **Y.-S. Song**, None; **T. Takahashi**, None; **A. Yoshida**, None

References

1. Early Treatment Diabetic Retinopathy Study Research Group. Grading diabetic retinopathy from stereoscopic color fundus photographs—an extension of the modified Airlie House classification. ETDRS report number 10. *Ophthalmology*. 1991;98:786–806.
2. Early Treatment Diabetic Retinopathy Study Research Group. Focal photocoagulation treatment of diabetic macular edema. Relationship of treatment effect to fluorescein angiographic and other retinal characteristics at baseline: ETDRS report no. 19. *Arch Ophthalmol*. 1995;113:1144–1155.
3. Early Treatment Diabetic Retinopathy Study Research Group. Treatment techniques and clinical guidelines for photocoagulation of diabetic macular edema. Early Treatment Diabetic Retinopathy Study Report Number 2. *Ophthalmology*. 1987; 94:761–774.
4. Early Treatment Diabetic Retinopathy Study Research Group. Classification of diabetic retinopathy from fluorescein angiograms. ETDRS report number 11. *Ophthalmology*. 1991;98: 807–822.
5. Yeung L, Lima VC, Garcia P, Landa G, Rosen RB. Correlation between spectral domain optical coherence tomography findings and fluorescein angiography patterns in diabetic macular edema. *Ophthalmology*. 2009;116:1158–1167.
6. Cho H, Alwassia AA, Regiatieri CV, et al. Retinal neovascularization secondary to proliferative diabetic retinopathy characterized by spectral domain optical coherence tomography. *Retina*. 2013;33:542–547.
7. Muqit MM, Stanga PE. Swept-source optical coherence tomography imaging of the cortical vitreous and the vitreoretinal interface in proliferative diabetic retinopathy: assessment of vitreoschisis neovascularisation and the internal limiting membrane. *Br J Ophthalmol*. 2014;98:994–997.
8. Muqit MM, Stanga PE. Fourier-domain optical coherence tomography evaluation of retinal and optic nerve head neovascularisation in proliferative diabetic retinopathy. *Br J Ophthalmol*. 2014;98:65–72.
9. Lee CS, Lee AY, Sim DA, et al. Reevaluating the definition of intraretinal microvascular abnormalities and neovascularization elsewhere in diabetic retinopathy using optical coherence tomography and fluorescein angiography. *Am J Ophthalmol*. 2015;159:101–110.e101.
10. Vaz-Pereira S, Zarranz-Ventura J, Sim DA, et al. Optical coherence tomography features of active and inactive retinal neovascularization in proliferative diabetic retinopathy. *Retina*. 2016;36:1132–1142.
11. Mariampillai A, Standish BA, Moriyama EH, et al. Speckle variance detection of microvasculature using swept-source optical coherence tomography. *Opt Lett*. 2008;33:1530–1532.
12. Miura M, Makita S, Iwasaki T, Yasuno Y. Three-dimensional visualization of ocular vascular pathology by optical coherence angiography in vivo. *Invest Ophthalmol Vis Sci*. 2011;52: 2689–2695.
13. Jia Y, Tan O, Tokayer J, et al. Split-spectrum amplitude-decorrelation angiography with optical coherence tomography. *Opt Express*. 2012;20:4710–4725.
14. Schwartz DM, Fingler J, Kim DY, et al. Phase-variance optical coherence tomography: a technique for noninvasive angiography. *Ophthalmology*. 2014;121:180–187.
15. Spaide RF, Klancnik JM Jr, Cooney MJ. Retinal vascular layers imaged by fluorescein angiography and optical coherence tomography angiography. *JAMA Ophthalmol*. 2015;133:45–50.
16. Huang Y, Zhang Q, Thorell MR, et al. Swept-source OCT angiography of the retinal vasculature using intensity differentiation-based optical microangiography algorithms. *Ophthalmic Surg Lasers Imaging Retina*. 2014;45:382–389.
17. Miura M, Hong YJ, Yasuno Y, Muramatsu D, Iwasaki T, Goto H. Three-dimensional vascular imaging of proliferative diabetic retinopathy by Doppler optical coherence tomography. *Am J Ophthalmol*. 2015;159:528–538.e523.
18. Kuehlewein L, Bansal M, Lenis TL, et al. Optical coherence tomography angiography of type 1 neovascularization in age-related macular degeneration. *Am J Ophthalmol*. 2015;160: 739–748.e732.
19. Jia Y, Bailey ST, Hwang TS, et al. Quantitative optical coherence tomography angiography of vascular abnormalities in the living human eye. *Proc Natl Acad Sci U S A*. 2015;112: E2395–E2402.
20. Matsunaga DR, Yi JJ, De Koo LO, Ameri H, Puliafito CA, Kashani AH. Optical coherence tomography angiography of diabetic retinopathy in human subjects. *Ophthalmic Surg Lasers Imaging Retina*. 2015;46:796–805.
21. Hwang TS, Jia Y, Gao SS, et al. Optical coherence tomography angiography features of diabetic retinopathy. *Retina*. 2015;35: 2371–2376.

22. Zhang Q, Lee CS, Chao J, et al. Wide-field optical coherence tomography based microangiography for retinal imaging. *Sci Rep*. 2016;6:22017.
23. de Carlo TE, Bonini Filho MA, Baumal CR, et al. Evaluation of preretinal neovascularization in proliferative diabetic retinopathy using optical coherence tomography angiography. *Ophthalmic Surg Lasers Imaging Retina*. 2016;47:115–119.
24. Ishibazawa A, Nagaoka T, Takahashi A, et al. Optical coherence tomography angiography in diabetic retinopathy: a prospective pilot study. *Am J Ophthalmol*. 2015;160:35–44.e1.
25. Spaide RF. Optical coherence tomography angiography signs of vascular abnormalization with antiangiogenic therapy for choroidal neovascularization. *Am J Ophthalmol*. 2015;160:6–16.
26. Wilkinson CP, Ferris FL III, Klein RE, et al. Proposed international clinical diabetic retinopathy and diabetic macular edema disease severity scales. *Ophthalmology*. 2003;110:1677–1682.
27. Miller H, Miller B, Zonis S, Nir I. Diabetic neovascularization: permeability and ultrastructure. *Invest Ophthalmol Vis Sci*. 1984;25:1338–1342.
28. Aiello LP, Avery RL, Arrigg PG, et al. Vascular endothelial growth factor in ocular fluid of patients with diabetic retinopathy and other retinal disorders. *N Engl J Med*. 1994;331:1480–1487.
29. Ogata N, Nishikawa M, Nishimura T, Mitsuma Y, Matsumura M. Unbalanced vitreous levels of pigment epithelium-derived factor and vascular endothelial growth factor in diabetic retinopathy. *Am J Ophthalmol*. 2002;134:348–353.
30. Avery RL, Pearlman J, Pieramici DJ, et al. Intravitreal bevacizumab (Avastin) in the treatment of proliferative diabetic retinopathy. *Ophthalmology*. 2006;113:1695–1705.e6.
31. Spaide RF, Fisher YL. Intravitreal bevacizumab (Avastin) treatment of proliferative diabetic retinopathy complicated by vitreous hemorrhage. *Retina*. 2006;26:275–278.
32. Kuiper EJ, Van Nieuwenhoven FA, de Smet MD, et al. The angio-fibrotic switch of VEGF and CTGF in proliferative diabetic retinopathy. *PLoS One*. 2008;3:e2675.
33. El-Sabagh HA, Abdelghaffar W, Labib AM, et al. Preoperative intravitreal bevacizumab use as an adjuvant to diabetic vitrectomy: histopathologic findings and clinical implications. *Ophthalmology*. 2011;118:636–641.
34. Sogawa K, Nagaoka T, Ishibazawa A, Takahashi A, Tani T, Yoshida A. En-face optical coherence tomography angiography of neovascularization elsewhere in hemicentral retinal vein occlusion. *Int Med Case Rep J*. 2015;8:263–266.
35. Davis MD, Blodi BA. *Proliferative Diabetic Retinopathy*. 4th ed. Philadelphia, PA: Elsevier; 2006.

Investigative Ophthalmology & Visual Science